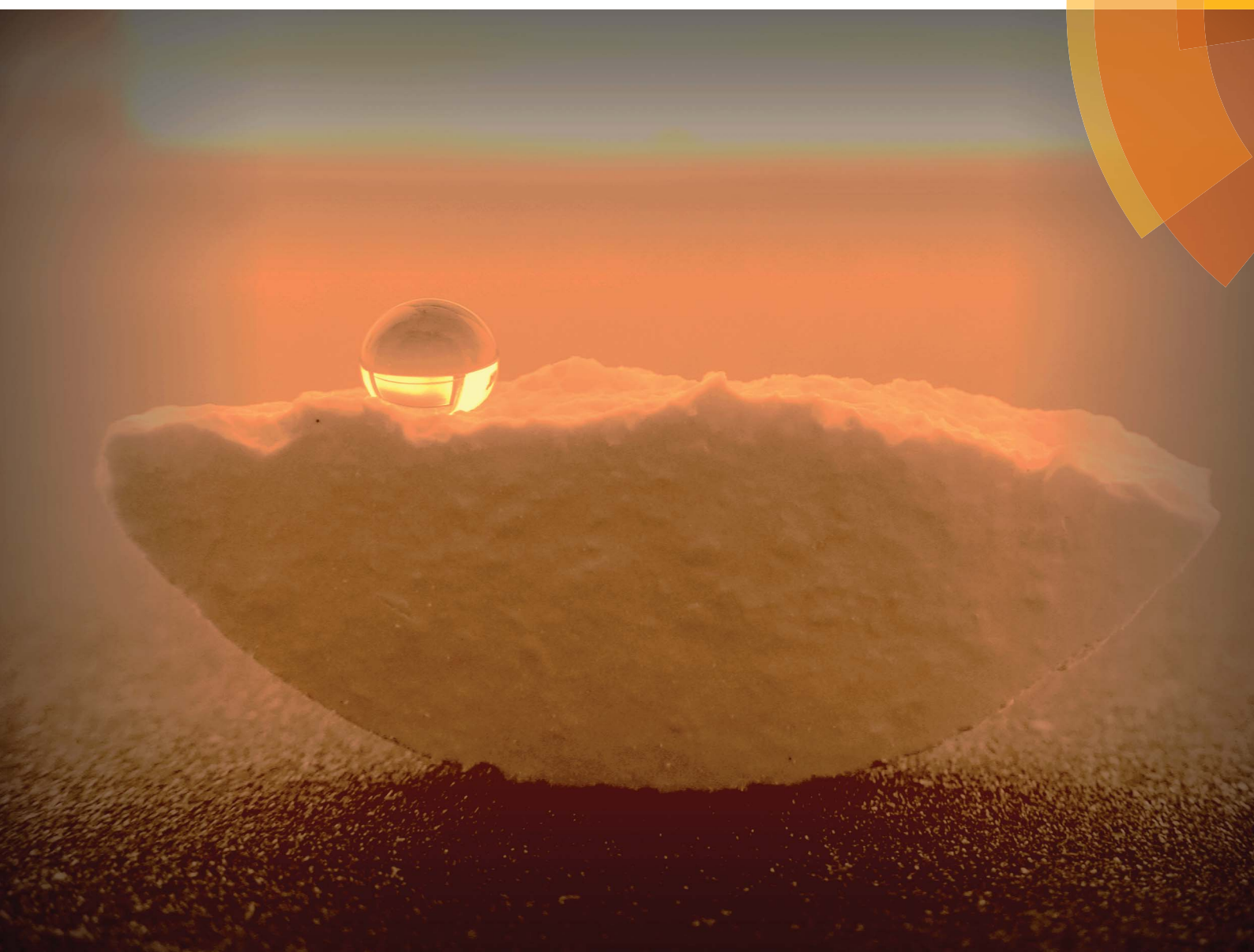


# Journal of Materials Chemistry A

Materials for energy and sustainability

[rsc.li/materials-a](http://rsc.li/materials-a)



ISSN 2050-7488



## PAPER

Manish K. Tiwari, Yao Lu *et al.*

Super-durable, non-fluorinated superhydrophobic free-standing items



Cite this: *J. Mater. Chem. A*, 2018, **6**, 357

## Super-durable, non-fluorinated superhydrophobic free-standing items†

Xia Zhang,  <sup>a</sup> Danfeng Zhi, <sup>a</sup> Lei Sun, <sup>a</sup> Yanbao Zhao, <sup>a</sup> Manish K. Tiwari,  <sup>\*b</sup> Claire J. Carmalt,  <sup>c</sup> Ivan P. Parkin <sup>c</sup> and Yao Lu  <sup>\*b</sup>

Although superhydrophobic coatings are commercially available, their weak mechanical durability hinders their large-scale applications such as for structural materials. Here a general press-in-mold method is reported to rapidly fabricate super-robust and non-fluorinated superhydrophobic free-standing items, through dispersing hydrophobic  $\text{SiO}_2$  nanoparticles in a series of polymers. The mechanical and chemical strength can be greatly improved by increasing the fabrication pressure, and the materials are found to retain superhydrophobicity after a knife/file scratch test, a liquid nitrogen test, severe sand/water impacts, acidic/alkali corrosion and 2000 cm sandpaper abrasion. These materials achieved better abrasion resistance than commercial superhydrophobic coatings and a higher retention ratio after abrasion tests and hardness than those of bricks. Radar diagrams were used to generalize the results of the mechanical and chemical tests to compare the material performances of  $\text{SiO}_2$ /polymer blocks with those of bricks and commercial superhydrophobic coatings. The  $\text{SiO}_2$ /polymer blocks achieved much better overall performance. This simple method has great potential for making either small domestic items or structural materials with robust superhydrophobicity.

Received 9th October 2017  
Accepted 9th November 2017

DOI: 10.1039/c7ta08895g  
[rsc.li/materials-a](http://rsc.li/materials-a)

Superhydrophobic surfaces are inspired by the Lotus leaf in nature,<sup>1</sup> which has excellent properties of self-cleaning,<sup>2</sup> oil-water separation,<sup>3</sup> and anti-corrosion.<sup>4</sup> Although artificial superhydrophobic coatings are commercially available, these coatings still lose their functions after mechanical abrasion. This is because the fabrication of superhydrophobic coatings involves creating a micro/nano-scale rough surface morphology and functionalizing the surface structures to lower their surface energy.<sup>5</sup> However, micro/nano-scale surface structures are inherently fragile and are easily removed, leading to the loss of superhydrophobicity.

To date, there are three strategies that are usually used to improve the mechanical robustness of superhydrophobic surfaces. Strategy 1 is to bond functionalized hydrophobic nanoparticles and adhesives.<sup>6</sup> This strategy is widely applied for some commercial superhydrophobic coatings such as the “NeverWet” spray – the surface robustness is highly dependent on the durability of the adhesives. Strategy 2 is to apply a substrate which is inherently abrasion-resistant for

superhydrophobic coatings, for example, when a flexible textile<sup>7</sup> or concrete<sup>8</sup> is used for the substrate. However, this strategy is limited by substrate materials. Strategy 3 is to disperse hydrophobic nanoparticles in polymers to make a thick superhydrophobic film;<sup>9</sup> in this system, a new layer of the film is present when the previous layer is worn out so that the superhydrophobicity remains. However, the wearability of these coatings mainly depends on the nature of the polymer, and it is difficult to further improve the mechanical robustness of these superhydrophobic coatings. Although the three strategies help improve the robustness of superhydrophobic coatings, the mechanical durability of the surface, as a coating, is also dependent on the strength of bonding between the substrate and the superhydrophobic coating.

In terms of lowering the surface energy, poly- or perfluoroalkyl hydrophobic agents are used in most superhydrophobic surfaces;<sup>10</sup> this is because fluorocarbons have lower water affinity even compared with hydrophobic hydrocarbons.<sup>11</sup> However, fluorinated surfaces are also considered to have environmental issues due to their potential threats to human health.<sup>12</sup>

Free-standing items are everywhere and of great importance to our daily life, such as bricks. Making the full body of free-standing materials superhydrophobic allows them to retain their properties after abrasion as the superhydrophobic material is throughout the bulk and not just confined to the surface. However, the superhydrophobicity of these free-standing materials may reduce their mechanical strength,<sup>8</sup> which may

<sup>a</sup>National & Local Joint Engineering Research Center for Applied Technology of Hybrid Nanomaterials, Henan University, Kaifeng 475004, P. R. China

<sup>b</sup>Nanoengineered Systems Laboratory, UCL Mechanical Engineering, University College London, London, WC1E 7JE, UK. E-mail: [yao.lu@ucl.ac.uk](mailto:yao.lu@ucl.ac.uk); [m.tiwari@ucl.ac.uk](mailto:m.tiwari@ucl.ac.uk)

<sup>c</sup>Department of Chemistry, University College London, 20 Gordon Street, London, WC1H 0AJ, UK

† Electronic supplementary information (ESI) available. See DOI: [10.1039/c7ta08895g](https://doi.org/10.1039/c7ta08895g)



even lead to a greater wear rate in abrasion than the untreated materials.

Here, we present a general method to fabricate super-robust and non-fluorinated superhydrophobic blocks through compressing nanoparticles and a series of polymers. These free-standing blocks are independent of substrates and show high abrasion-resistant properties. The mechanical and chemical stability and hardness can be further improved by increasing the compression pressure during the fabrication process. The superhydrophobic blocks show superior mechanical robustness compared with commercial superhydrophobic coatings with a higher retention ratio and hardness greater than those of household bricks after sandpaper abrasion for 2000 cm.

To prepare durable superhydrophobic free-standing blocks, we pressed a hydrophobic  $\text{SiO}_2$  nanoparticles–polymer matrix in a mold at 5, 10, 30 and 40 MPa, respectively. The hydrophobic  $\text{SiO}_2$  nanoparticles were prepared by treating  $\text{SiO}_2$  nanoparticles with hexamethyldisilazane (HMDS) using a literature method.<sup>13</sup> The hydrophobic  $\text{SiO}_2$  nanoparticles were well dispersed in polyhexamethylene adipamide (PA610), polystyrene (PS), polypropylene (PP), and methyl silicone resin (MSR), respectively. After drying, the samples became  $\text{SiO}_2$ /polymer composites, and then they were fabricated into hard free-standing blocks after being pressed in a mold. These blocks became superhydrophobic after being manually abraded 2 to 3 times by using

sandpaper ( $\text{SiC}$ , 800 Cw). The whole fabrication process did not include any fluorinated polymers so that the materials can be considered to be potentially safer to human health than those from many recent research methods.<sup>14</sup>

Fig. 1 shows the optical images, scanning electron microscope (SEM) images, and X-ray photoelectron spectroscopy (XPS) and thermogravimetric (TG) analysis of the  $\text{SiO}_2$ /polymer blocks. Samples were fabricated at 30 MPa throughout the experiments unless otherwise specified. The water contact angles (WCAs) of the  $\text{SiO}_2$ -PA610, PS, PP, and MSR surfaces were all greater than  $150^\circ$  showing their superhydrophobicity.<sup>15</sup> After being slightly abraded, the SEM images show that the samples have micro/nano-surface morphologies that are required for superhydrophobicity. XPS analysis shows that these blocks mainly consist of C, O and Si, and do not contain any fluorinated materials. TG analysis demonstrates that these  $\text{SiO}_2$ /polymer blocks were stable up to  $200^\circ\text{C}$ ; this would meet most of the domestic requirements.

To evaluate the mechanical robustness of the samples, we performed a series of mechanical tests on the  $\text{SiO}_2$ /polymer blocks as shown in Fig. 2. We performed knife scratch and file abrasion tests on the  $\text{SiO}_2$ /PP blocks both in air and in water, as shown in Fig. 2a–d, and it was observed that the samples retained superhydrophobicity after these tests as well as fingerprint and tape peeling tests as shown in Movies S1–S4.†

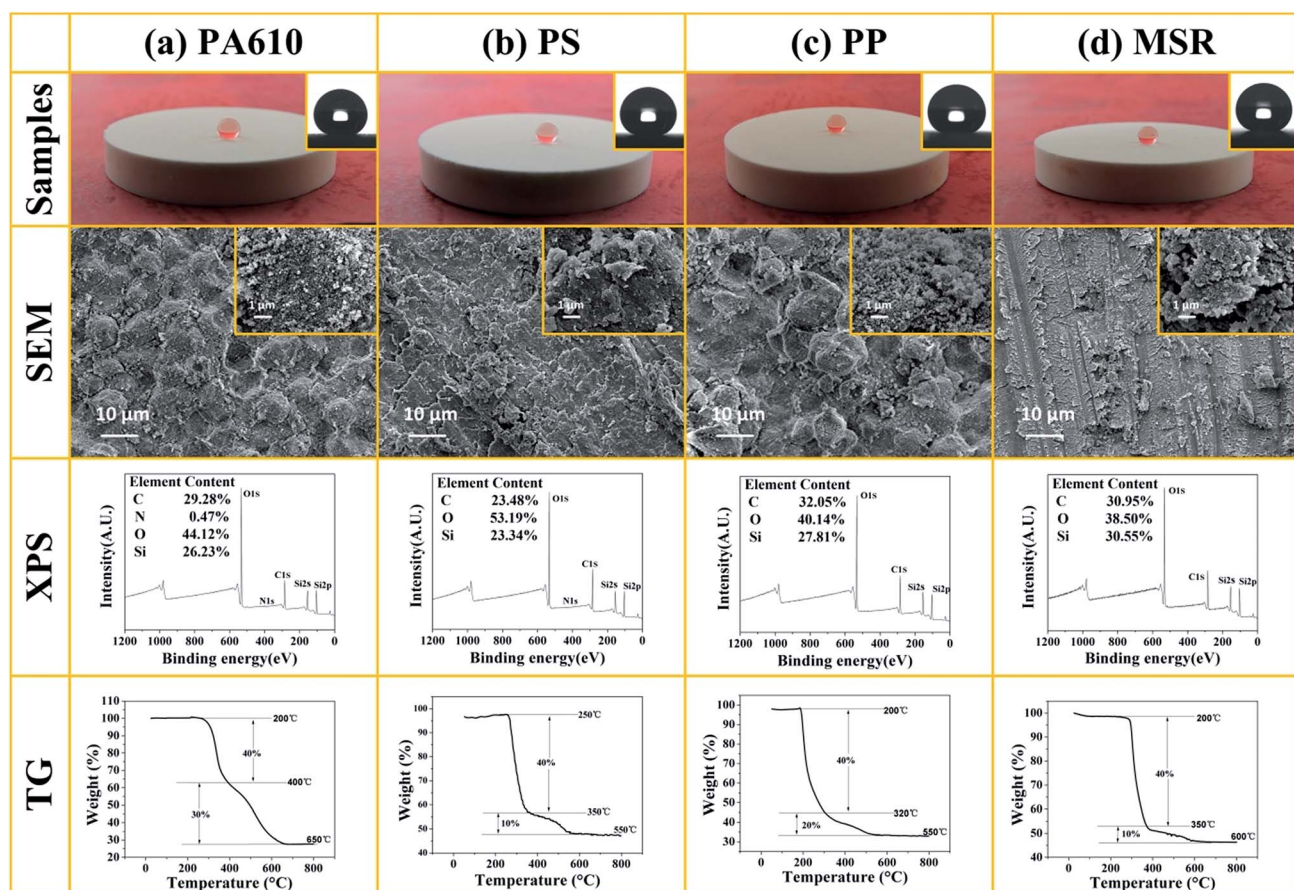


Fig. 1 Optical and SEM images, and XPS and TG analysis of the  $\text{SiO}_2$ /polymer blocks. Water droplets were dyed red with cobalt(II) nitrate hexahydrate to aid visualization and this did not change the wetting behavior of water.

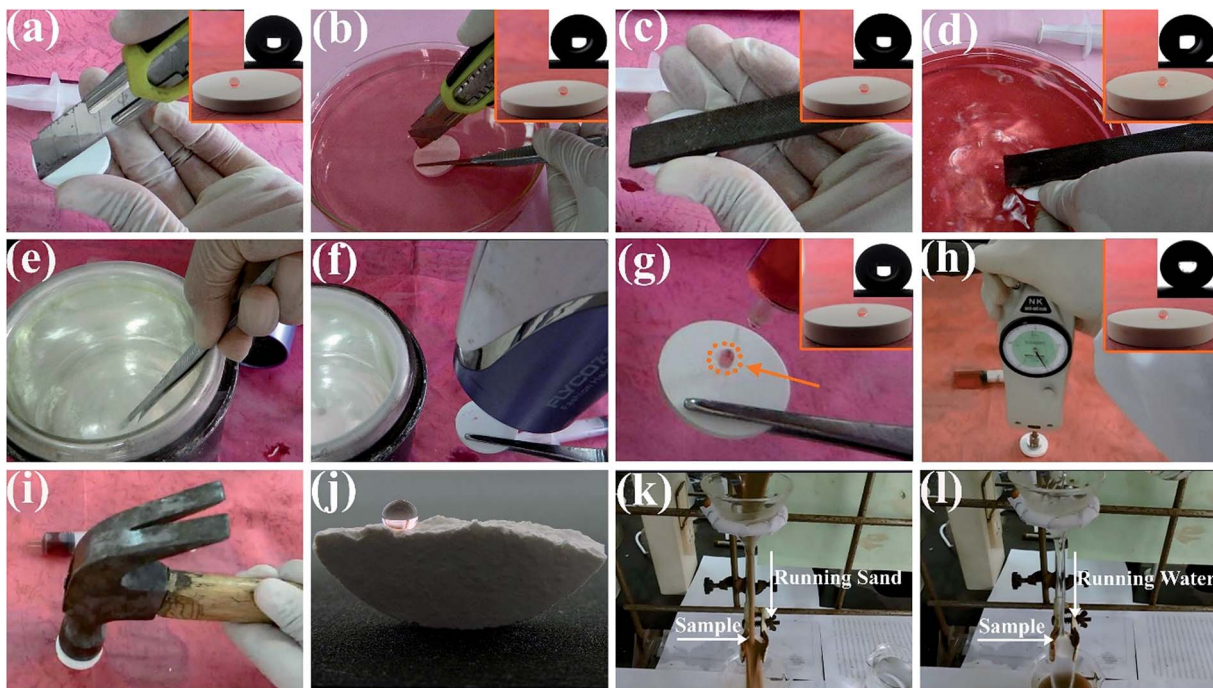


Fig. 2 (a)–(g) Mechanical tests on the  $\text{SiO}_2/\text{PP}$  block. (a) Knife scratch test in air. (b) Knife scratch test in water. (c) File abrasion test in air. (d) File abrasion test in water. (e)–(g) Liquid nitrogen tests. (h)–(l) Mechanical tests on the  $\text{SiO}_2/\text{PA610}$  block. (h) Newton meter press test at  $\sim 200$  N. (i) and (j) Hammer beat and the droplet test at the cross-sectional crack to show superhydrophobicity inside the material. (k) and (l) Running sand impacts followed by running water rinsing. Insets show the wettability of the sample after the corresponding tests.

To test the recovery ability after being exposed to extremely low temperatures, a liquid nitrogen test is usually applied.<sup>16</sup> Fig. 2e–g and Movie S5† show that the  $\text{SiO}_2/\text{PP}$  block was dipped into liquid nitrogen for  $\sim 10$  s and then removed. Water (dyed with cobalt(II) nitrate hexahydrate to aid visualization) was added dropwise and frozen on the sample, and then a hair dryer was used to heat the sample and the frozen droplets. After the heating process, there were some stains of the dye powder on the sample; water was then added dropwise onto the sample and the stains were easily removed, indicating that the superhydrophobicity was recovered. Fig. 2h and Movie S6† show that after the  $\text{SiO}_2/\text{PA610}$  sample was pressed at  $\sim 200$  N, it retained superhydrophobicity, indicating its mechanical robustness. The  $\text{SiO}_2/\text{PA610}$  sample was broken by using a hammer (Fig. 2i, j and Movie S7†), and the broken area retained superhydrophobicity, indicating that even the inside parts of the blocks repel water. Fig. 2k, l and Movie S8† show the sand–water impact tests. The  $\text{SiO}_2/\text{PA610}$  block was strongly impacted by dropping sand followed by running water, and the surface remained dry and clean after these tests.

The aforementioned tests give an understanding of the mechanical robustness of the  $\text{SiO}_2/\text{polymer}$  blocks. To further quantify the abrasion-resistance of these materials, we plotted the WCA, water sliding angle (WSA) and retention ratio as functions of the abrasion distance as shown in Fig. S1.† The retention ratio  $\eta = m_1/m_2 \times 100\%$ , where  $m_1$  refers to the sample mass after abrasion for a distance, and  $m_2$  refers to the original sample mass. In this test, the samples were loaded with an 80 g weight with an area of  $7.065 \text{ cm}^2$ , and the original weight

of these samples before abrasion was  $2 \pm 0.3$  g. The  $\text{SiO}_2/\text{polymer}$  blocks were abraded on sandpaper (SiC, 1000 Cw) for 2000 cm, and most of the samples retained superhydrophobicity after abrasion. At a higher fabrication pressure, there was a higher retention ratio for the four samples, indicating that less material was worn out. This is because the materials were made more condensed and robust at a higher fabrication pressure (40 MPa), leading to a higher retention ratio, so that high WCAs and low WSAs were retained after 2000 cm abrasion. The wettability of these samples did not show significant differences as their WCAs ranged from  $149.5^\circ$  (PS block after 2000 cm abrasion) to  $164.5^\circ$  (MSR block before abrasion), and this is related to the fact that their surface morphologies did not significantly change before and after abrasion for 2000 cm travel as shown in Fig. S2.† To understand the required roughness for superhydrophobicity, we used a friction tribotester with the pin-on-disk configuration (Fig. S3a†) and used  $\text{SiO}_2/\text{PS}$  blocks as an example. The sample was positioned onto the lower disk, and sandpapers with different grits (SiC, 320, 600, 800, and 1200 Cw) were attached onto the upper stationary pins. The sample was abraded under a 40 g load at 60 rpm for 10 min. Fig. S3b† shows that the WCA retained a value of  $155^\circ$  with 320 Cw sandpaper abrasion but decreased to  $120^\circ$  when much finer sandpaper was applied (1200 Cw). The coefficient of friction (COF) became stable after 1 min abrasion (Fig. S3c†) and superhydrophobicity ( $\text{WCA} > 150^\circ$ ) was achieved when the surface roughness  $R_a$  was greater than  $3.0 \mu\text{m}$  (Fig. S3d†). Fig. S3e–l† show the SEM images of the samples after abrasion by using sandpapers of grits 320, 600,



800, and 1200 Cw, respectively. They show that the surfaces were more textured after abrasion using coarse sandpapers (grits 320, 600, and 800 Cw), and this was less dependent on the abrasion distance according to Fig. S1 and S2.<sup>†</sup> When fine sandpaper (1200 Cw) was applied, the surfaces were smooth and lost superhydrophobicity. Using the same setup of the tribotester, we loaded different weights of 20, 40, 60, and 80 g onto the  $\text{SiO}_2/\text{PS}$  blocks for sandpaper abrasion (800 Cw). The COF was stable after 1 min abrasion (Fig. S4a<sup>†</sup>) and

superhydrophobicity was achieved when the surface roughness  $R_a$  was greater than 3.0  $\mu\text{m}$  (Fig. S4b<sup>†</sup>), indicating that the relationship between  $R_a$  and wettability is constant for the  $\text{SiO}_2/\text{PS}$  sample. Fig. S4c–f<sup>†</sup> show the SEM images of the samples after abrasion; the finest abrasion was achieved when a 20 g weight was loaded.

Chemical stability is also a very important characteristic of superhydrophobic materials.<sup>17</sup> We performed two independent experiments to study the chemical durability of these  $\text{SiO}_2/$

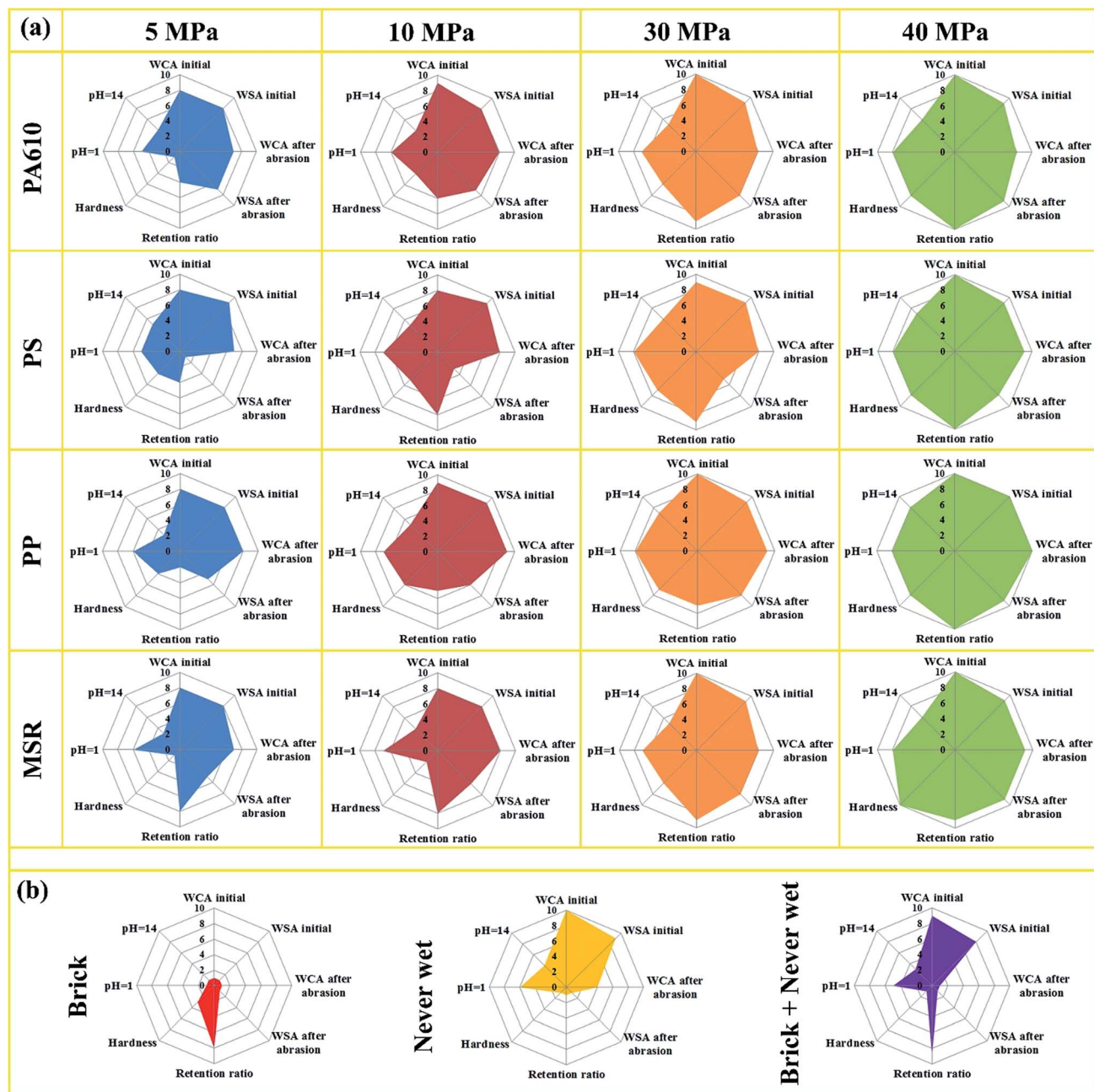


Fig. 3 Radar diagrams of the  $\text{SiO}_2/\text{polymer}$  blocks, a brick and the "Never wet" commercial superhydrophobic spray. Here, "WCA initial" and "WSA initial" refer to the water contact angles and water sliding angles of the samples before any mechanical and chemical tests. "WCA after abrasion" and "WSA after abrasion" refer to the water contact angles and water sliding angles that were measured after the samples being abraded for 2000 cm (80 g loads, SiC, 1000 Cw sandpaper). Retention ratio data were collected from the samples after 2000 cm abrasion (80 g loads, SiC, 1000 Cw sandpaper). "pH = 1" and "pH = 14" refer to the contact angles that were measured after a 30 min "droplet test". Hardness was measured for the samples before any tests.



polymer blocks. In the “droplet test”, strong acid ( $\text{pH} = 1$ ) and alkali ( $\text{pH} = 14$ ) droplets were positioned onto the  $\text{SiO}_2$ /polymer blocks for 30 min as shown in Fig. S5,† and note that the water droplets became smaller due to evaporation. As the acid/alkali contact time increased, the CAs of the acid/alkali droplets slightly decreased but still remained at  $\sim 150^\circ$ . In a more aggressive test, the samples were immersed in acid ( $\text{pH} = 1$ ) and alkali ( $\text{pH} = 14$ ) baths for 30 min, and WCAs were measured every 5 min of soaking time, as shown in Fig. S5.† Although the WCAs decreased from  $\sim 160^\circ$  to  $\sim 150^\circ$ , the  $\text{SiO}_2$ /polymer blocks retained their superhydrophobicity.

To give an overview of the mechanical and chemical durability of the  $\text{SiO}_2$ /polymer blocks and compare them with bricks and commercial superhydrophobic surfaces, we used radar diagrams to evaluate the experimental data as shown in Fig. 3.<sup>18</sup> In the radar diagrams, we included WCAs and WSAs before and after sandpaper abrasion (SiC, 1000 Cw, 80 g loading, and 2000 cm abrasion), the retention ratio after 2000 cm abrasion, and WCAs after the “droplet tests” for 30 min; the hardness of the samples was included and measured using a shore hardness durometer (Type A). Table S1† shows the rating system of the radar diagram according to the performance of the samples, and their datasheets are as shown in Tables S2–S6;† the average values of the datasheets were used in the radar diagram. The larger area of the radar diagram indicates better performance. As the fabrication pressure increased, all the performances improved including chemical and mechanical stability, and hardness. Although corrosive liquids made bigger impacts on these blocks than mechanical abrasion did, the 40 MPa fabricated samples still showed significant chemical resistance. With the more condensed characteristic of the 40 MPa pressed blocks, the retention ratio and hardness were even larger than those of household bricks, indicating that these composites have the potential to replace bricks with superhydrophobic properties. The blocks show superior chemical and mechanical abrasion resistance compared with commercial superhydrophobic sprays (Never wet) and Never wet coated bricks.

In conclusion, a general press-in-mold method was developed to make super-durable and non-fluorinated superhydrophobic free-standing items using hydrophobic  $\text{SiO}_2$  nanoparticles and various polymers. The mechanical and chemical properties were much better than those of commercial superhydrophobic coatings and bricks, and could be greatly improved with an increase of the fabrication pressure. The superhydrophobicity of 40 MPa fabricated blocks was retained even after 2000 cm abrasion and 30 min acid/alkali corrosion. More durable materials could be achieved given higher fabrication pressure, and various shapes of free-standing items could be fabricated when different molds were applied. This method provides a new approach to making super-robust and non-fluorinated superhydrophobic materials for domestic items and building new structural materials. These composite bricks have real potential in stopping water permeation.

## Conflicts of interest

There are no conflicts of interest to declare.

## Acknowledgements

This work was supported by the National Natural Science Foundation of China (Grant No. 21403055, 21711530209) and Joint Talent Cultivation Funds of NSFC-HN (Grant No. U1304529). Y. Lu and M. K. Tiwari acknowledge the support from the EPSRC project EP/N024915/1. I. P. Parkin acknowledges the EPSRC M3S CDT grant (EP/L015862/1).

## References

- 1 (a) W. Barthlott and C. Neinhuis, *Planta*, 1997, **202**, 1; (b) H. J. Lee and S. Michielsen, *J. Text. Inst.*, 2006, **97**, 455; (c) A. Marmur, *Langmuir*, 2004, **20**, 3517.
- 2 (a) R. Fürstner, W. Barthlott, C. Neinhuis and P. Walzel, *Langmuir*, 2005, **21**, 956; (b) B. Bhushan and Y. C. Jung, *Prog. Mater. Sci.*, 2011, **56**, 1.
- 3 (a) Y. Lu, S. Sathasivam, J. Song, F. Chen, W. Xu, C. J. Carmalt and I. P. Parkin, *J. Mater. Chem. A*, 2014, **2**, 11628; (b) Z. Xue, Y. Cao, N. Liu, L. Feng and L. Jiang, *J. Mater. Chem. A*, 2014, **2**, 2445.
- 4 (a) H. Qian, D. Xu, C. Du, D. Zhang, X. Li, L. Huang, L. Deng, Y. Tu, J. M. C. Mol and H. A. Terryn, *J. Mater. Chem. A*, 2017, **5**, 2355; (b) T. Rezayi and M. H. Entezari, *Surf. Coat. Technol.*, 2017, **309**, 795.
- 5 B. Wang, J. Li, G. Wang, W. Liang, Y. Zhang, L. Shi, Z. Guo and W. Liu, *ACS Appl. Mater. Interfaces*, 2013, **5**, 1827.
- 6 Y. Lu, S. Sathasivam, J. Song, C. R. Crick, C. J. Carmalt and I. P. Parkin, *Science*, 2015, **347**, 1132.
- 7 (a) J. Zimmermann, F. A. Reifler, G. Fortunato, L. C. Gerhardt and S. Seeger, *Adv. Funct. Mater.*, 2008, **18**, 3662; (b) X. Zhou, Z. Zhang, X. Xu, F. Guo, X. Zhu, X. Men and B. Ge, *ACS Appl. Mater. Interfaces*, 2013, **5**, 7208.
- 8 J. Song, D. Zhao, Z. Han, W. Xu, Y. Lu, X. Liu, B. Liu, C. J. Carmalt, X. Deng and I. P. Parkin, *J. Mater. Chem. A*, 2017, **5**, 14542.
- 9 (a) N. Wang, Y. Lu, D. Xiong, C. J. Carmalt and I. P. Parkin, *J. Mater. Chem. A*, 2016, **4**, 4107; (b) Q. Ke, W. Fu, H. Jin, L. Zhang, T. Tang and J. Zhang, *Surf. Coat. Technol.*, 2011, **205**, 4910.
- 10 (a) J. Y. Huang, S. H. Li, M. Z. Ge, L. N. Wang, T. L. Xing, G. Q. Chen, X. F. Liu, S. S. Al-Deyab, K. Q. Zhang and T. Chen, *J. Mater. Chem. A*, 2015, **3**, 2825; (b) S. Chen, X. Li, Y. Li and J. Sun, *ACS Nano*, 2015, **9**, 4070; (c) Y. Wang, J. Xue, Q. Wang, Q. Chen and J. Ding, *ACS Appl. Mater. Interfaces*, 2013, **5**, 3370.
- 11 V. H. Dalvi and P. J. Rossky, *Proc. Natl. Acad. Sci. U. S. A.*, 2010, **107**, 13603.
- 12 (a) J. Ju, X. Yao, X. Hou, Q. Liu, Y. S. Zhang and A. Khademhosseini, *J. Mater. Chem. A*, 2017, **5**, 16273; (b) X. C. Hu, D. Q. Andrews, A. B. Lindstrom, T. A. Bruton, L. A. Schaider, P. Grandjean, R. Lohmann, C. C. Carignan, A. Blum and S. A. Balan, *Environ. Sci. Technol. Lett.*, 2016, **3**, 344; (c) J. W. Martin, D. M. Whittle, D. C. G. Muir and S. A. Mabury, *Environ. Sci. Technol.*, 2004, **38**, 5379.
- 13 D. Zhi, Y. Lu, S. Sathasivam, I. P. Parkin and X. Zhang, *J. Mater. Chem. A*, 2017, **5**, 10622.



14 (a) Y. Qing, C. Yang, N. Yu, Y. Shang, Y. Sun, L. Wang and C. Liu, *Chem. Eng. J.*, 2016, **290**, 37; (b) F. Chen, J. Song, Y. Lu, S. Huang, X. Liu, J. Sun, C. J. Carmalt, I. P. Parkin and W. Xu, *J. Mater. Chem. A*, 2015, **3**, 20999.

15 (a) J. Heikenfeld and M. Dhindsa, *J. Adhes. Sci. Technol.*, 2008, **22**, 319; (b) J. Tam, Z. Jiao, J. C. F. Lau and U. Erb, *Wear*, 2017, **374**, 1.

16 Y. Lu, G. He, C. J. Carmalt and I. P. Parkin, *RSC Adv.*, 2016, **6**, 106491.

17 (a) Q. Liu, D. Chen and Z. Kang, *ACS Appl. Mater. Interfaces*, 2015, **7**, 1859; (b) J. Zimmermann, G. R. J. Artus and S. Seeger, *Appl. Surf. Sci.*, 2007, **253**, 5972.

18 A. Wojdyła, A. Taylor, G. Durand and I. W. Boyd, *Wear*, 2017, **390**, 49.